electrochem

MDPI

Article

Low-Volume Electrochemical Sensor Platform for Direct Detection of Paraquat in Drinking Water

Durgasha C. Poudyal [1], Manish Samson [1], Vikram Narayanan Dhamu [2], Sera Mohammed [1], Claudia N. Tanchez [1], Advaita Puri [1], Diya Baby [1], Sriram Muthukumar [2] and Shalini Prasad [1,2,*]

[1] Department of Bioengineering, University of Texas at Dallas, Richardson, TX 75080, USA
[2] EnLiSense LLC, Allen, TX 75013, USA
* Correspondence: shalini.prasad@utdallas.edu; Tel.: +1-(972)-883-4247

Abstract: Direct testing of pesticide contaminants in drinking water is a challenge. Portable and sensitive sensor platforms are desirable to test water contaminants directly at farm and consumer levels. In this study, we have demonstrated the feasibility of an electrochemical sensor for the direct detection of paraquat (PQ) in drinking water samples. An immunoassay-based sensing platform was fabricated using PQ-specific antibody immobilized on the surface of the electrochemically reduced graphene oxide (rGO) modified screen-printed carbon electrode (rGO-SPCE). Using non-faradaic electrochemical impedance spectroscopy (EIS) as a detection tool, the sensor platform demonstrated a dynamic response for PQ concentration in drinking water ranging from 0.05 ng/mL to 72.9 ng/mL (0.19 to 243.8 nM), with a coefficient of determination (r^2) of 0.997 and a limit of detection of 0.05 ng/mL (0.19 nM). Percentage recovery within ±20% error was obtained, and the sensor cross-reactivity test showed a selective response against glyphosate antigen. With the flexibility to use single-frequency EIS and low sample volume, the developed sensor demonstrated testing in water samples directly without any sample pre-processing. This low-volume electroanalytical sensor platforms can be translated into portable testing tools for the detection of various water contaminants.

Keywords: electrochemical sensors; electrochemical impedance spectroscopy (EIS); cyclic voltammetry; label-free detection; paraquat detection; pesticides in water

check for updates

Citation: Poudyal, D.C.; Samson, M.; Dhamu, V.N.; Mohammed, S.; Tanchez, C.N.; Puri, A.; Baby, D.; Muthukumar, S.; Prasad, S. Low-Volume Electrochemical Sensor Platform for Direct Detection of Paraquat in Drinking Water. *Electrochem* **2024**, *5*, 341–353. https://doi.org/10.3390/electrochem5030022

Academic Editor: Masato Sone

Received: 17 June 2024
Revised: 22 July 2024
Accepted: 16 August 2024
Published: 22 August 2024

Copyright: © 2024 by the authors. Licensee MDPI, Basel, Switzerland. This article is an open access article distributed under the terms and conditions of the Creative Commons Attribution (CC BY) license (https://creativecommons.org/licenses/by/4.0/).

1. Introduction

Paraquat or 1,1-dimethyl-4,4-bipyridine dichloride, is a herbicide that is commonly used in a variety of applications encompassing weed control and crop desiccants [1]. Paraquat (PQ), which is also known by the name of methyl viologen, is an active component of dipyridine compounds and can be easily reduced into a free radical that is severely toxic to animals and humans [2,3]. PQ also has been known to cause severe necrosis to a variety of organ systems in humans, such as the lungs, kidneys, and heart, and can cause neurodegenerative diseases such as Parkinson's [4]. Due to the high effectiveness of PQ as well as its low unit cost, there is a significant overuse of PQ in agricultural applications, causing significant amounts of environmental pollution primarily in water. The maximum residue limit of PQ in water is between 3 and 200 nM [5,6]. Due to the low maximum residue limit in sources of water, detection methods need to be robust and reliable at low concentrations of PQ.

Various laboratory techniques are currently used for the detection of PQ, such as GC-MS, LC-MS, and HPLC-MS [7]. While these techniques yield accurate results, they require significant initial investment, intensive pre-sample processing, and trained technicians to reliably use the instruments and analyze results. All of these are significant barriers to entry for the democratization of reliable sensing of PQ, especially when usage is widespread. These laboratory techniques requiring phases of sample preparation, such as separation and purification, also inhibit point-of-care field sensing, containing sensing to a controlled,

sterile laboratory environment. Other alternatives such as surface-enhanced Raman spectroscopy were also investigated, especially since SERS is an analytical technique that is commonly used in trace pesticide detection [8]. However, one drawback that renders it difficult for usage by consumers is its dependency on instrumentation that is expensive and too sophisticated to properly handle. This dilemma highlights the need for a portable and highly sensitive sensing platform that can be used for in-field, point-of-care testing [9].

Historically, electrochemical sensors have high sensitivity, easy operation, low unit cost, and corresponding performance metrics to serve as reliable alternatives to laboratory analytical techniques [1,10–13]. However, the detection performance of such sensors depends on the surface of the working electrode, ease of usage, its sensitivity, and reproducibility. Therefore, modification of the transducer surface of the electrode is widely performed. Some examples of transducer materials include lead oxide nanoparticles, activated biochar (AB4), reduced graphene oxide (rGO), copper-based graphene oxide MOF, and an indium tin oxide electrode, which have all been successfully developed specifically for PQ detection [9,14–16]. While there have several reports on electrochemical sensors for the detection of PQ, the electrode surface modifications are complex and sample pretreatments are required, which limits the application of these sensors in real-time samples [17]. Therefore, another route needs to be explored to develop a sensitive and simple sensing platform for the detection of PQ that can be easily scaled and replicated on an industrial basis. With the development of screen-printing techniques and demand for portable sensor technology, the disposable carbon screen-printed electrode (SPE) has been rapidly developed to fabricate electrodes for electrochemical sensing applications [18]. Various surface modifications of SPE with two-dimensional materials, metal nanoparticles, and polymers have been explored to enhance the performance of SPE. However, graphene, another nanomaterial, has been utilized on screen-printed biosensors for a wide myriad of detection applications. Graphene-based material has been an emergent technology due to its exceptional chemical and physical properties [19]. Graphene oxide as a carbon-based layer strengthens contact between the two surfaces and amplifies the stability of the compound, allowing it to be used in a myriad of applications such as nanoelectronics and graphene-based electronics. A polypyrrole-grafted nitrogen-doped graphene (PPY-g-NGE) sensor was prepared for the detection of PQ and was able to determine the presence of PQ in samples at a detection limit of 41 nM [20–22]. Another application involving a PQ electrochemical sensor involved a graphene-paste electrode (SPGrE) modified with platinum nanoparticles. This electrochemical sensor was able to reliably gain a detection limit of 0.02 µM or 200 nM [20]. The formulation of these electrochemical sensors with graphene serving as the main modification for their sensing platform shows the promise of graphene as a nanomaterial and its ability to be used for the rapid detection of PQ utilizing other sensing mechanisms. Another approach is the immunoassay-based sensor modification approach, which is relatively simple and sensitive and allows for the rapid screening of large sample numbers on site. Using monoclonal antibodies, an immunochromatographic assay (ICA) was reported to determine PQ concentrations in water. The developed ICA method provided visible limits of detection ranging from 0.25 to 1 ng/mL, and cut-off limits ranging from 1 to 5 ng/mL [23]. Using polyclonal antibodies, several enzyme-linked immunosorbent assay (ELISA) methods have been established for PQ detection in food samples [23,24]. Utilizing an immunoassay-based electrochemical sensor for the detection of paraquat in drinking water has less explored. A comparison table consisting of various sensor platform response parameters, detection matrices, and detection limits is presented in Table S1 of Supplementary Information. Therefore, in this work, a simple immunosensor-based electrochemical sensor has been demonstrated. A screen-printed carbon electrode with electrochemically reduced graphene oxide as the transducer and support material, which was immobilized with PQ antibody (PQ-Ab) specific to the target antigen using a cross-linker. By formulating an interaction between nanomaterial, electrode surface, and antibody, the synergistic effect with these three elements amplifies the electrochemical sensor's detection capabilities. Coupled with the inherent ease of use and portability that

comes with electrochemical sensing, this sensing platform is aimed at allowing consumers to be able to detect the target analyte of PQ in water samples at very low concentrations to compare the gold-standard laboratory analytical techniques.

2. Experimental Section

2.1. Chemicals and Reagents

Commercial carbon screen-printed electrodes were procured from Metrohm DropSens, Riverview, FL, USA (ref 11L). The graphene oxide water dispersion of 4 mg/mL was procured from Graphenea (monolayer content > 95%). The paraquat polyclonal antibody used for sensor modification was procured from Invitrogen (PA1-85762, Rockford, IL, USA). Paraquat dichloride hydrate (PQ, ≥98.0%) 1-pyrenebutyricacid-N hydroxysuccinimide ester (PANHS, 95%), methanol (99+%), N-(Phosphonomethyl) glycine (GLY, ≥98.0%), and phosphate-buffered saline (pH 7.4) were procured from Sigma Aldrich, St. Louis, MO, USA. SuperBlock™ blocking buffer was procured from Thermo Scientific, Rockford, IL, USA. All the chemicals purchased were of analytical grade. All solutions used for experimentation were prepared using deionized water (DI, 18 MΩ cm^{-1} resistivity)

2.2. Instrumentation

Fourier-transform infrared spectroscopy (FTIR) scans were also recorded utilizing a Nicolet iS50 FTIR spectrometer, (Thermo Fisher Scientific, Madison, WI, USA with 256 spectral scans at a resolution of 4 cm^{-1} in the wavelength range of 4000 cm^{-1} to 600 cm^{-1} to confirm the binding of the cross-linker in tandem with the PQ antibody to the surface of the reduced graphene oxide screen-printed electrode. Atomic force microscopy (AFM) was performed using a Bruker Dimension Nano in Scan-Asyst mode(Bruker, Santa Barbara, CA, USA) to study the topography of modified sensor surface. AFM was performed directly on the surface of a modified immunoassay-based sensor to represent the actual surface after modification. All electrochemical benchtop measurements were recorded using a Gamry Reference 600 potentiostat (Gamry Instruments, Warminster, PA, USA). The electrodes used for this sensing platform were three electrode carbon SPEs from Metrohm Dropsens USA. All data and graphs were plotted utilizing GraphPad Prism version 10.3.0 (507) and Origin Pro 2024 (10.1.0.178).

2.3. Preparation of Sensor for the Detection of Paraquat

The sensor platform used in this study is a screen-printed electrode, and preparation involves the following steps.

2.3.1. Coating and In-Situ Electrochemical Reduction of Graphene Oxide (rGO) on Carbon Screen-Printed Electrode

The graphene oxide dispersion and electrochemical in-situ reduction were performed following a reported protocol with slight modifications [25–27]. A graphene water dispersion of concentration 1 mg/mL was exfoliated utilizing probe sonication for a period of 1 h followed by bath sonication for 15 min. After this was concluded, 8 µL of this solution was drop-casted onto the working electrode of the carbon SPE and the electrode was allowed to dry at room temperature. To reduce the graphene oxide to rGO, the prepared GO film on the SPE was reduced using cyclic voltammetry in phosphate-buffer solution (pH 6.5) at a potential window 0.1 to −1.2 V vs. Ag/AgCl and scan rate 50 mV/s for 10 cycles [27]. For comparison, the CV measurements were also recorded before and after reduction using PBS (pH 7.4) at a potential window from −0.6 to 0.6 V vs. Ag/AgCl at a scan rate of 50 mV/s. The PBS was removed, and the electrode was dried at room temperature and stored in a desiccator for further usage.

2.3.2. Cross-Linker and Paraquat Antibody (PQ-Ab) Immobilization Step

PANHS cross-linker (8 µL, 10 mM, dissolved in methanol) was dispensed onto the surface of the freshly prepared rGO/SPE electrode and incubated at room temperature for a period of 90 min while contained in a Faraday cage to shield from air impurities or excessive light [28]. After this period concluded, the electrode was washed twice with PBS with a pH of 7.4 to remove any unbound cross-linker. After this was completed, 8 µL of 200 µg/mL PQ antibody (PQ-Ab) was immediately dispensed and allowed to incubate for 30 min at room temperature. After 30 min, the electrode was rinsed with PBS to remove any excess unbounded antibody. Lastly, 8 µL of blocking buffer or superblock was dispensed on the surface of the electrode and allowed to incubate for a period of 10 min to reduce nonspecific binding. After the 10 min had concluded, the electrode was washed with PBS and stored at 4 degrees Celsius for further use. Fourier-transform infrared spectroscopy (FTIR) was recorded after each modification step to confirm the binding of the cross-linker and immobilization antibody to the cross-linker surface.

3. Results and Discussion

3.1. Sensor Characterizations

The synthesis of reduced graphene oxide (rGO) from graphite oxide is considered the most economical for large production; however, it involves chemical reductants such as hydrazine, ascorbic acid, hydriodic acid, and sodium borohydride [29]. The rGO produced is in dispersion and is drop-casted onto the electrode for further electrochemical applications, which makes it difficult for applications due to low solubility. Electrochemical methods are one of the green strategies to synthesize reduced graphene oxide that is under mild conditions and free from contaminants [29,30].

Following the protocol reported in the literature, we employed an in-situ electrochemical reduction of GO to rGO to achieve a stable rGO film on the sensor surface. In the electrochemical reduction, the graphene oxide film on the carbon screen-printed electrode was reduced under negative potential, forming an rGO coating on the working area of the electrode. Figure 1A shows the in-situ electrochemical reduction of graphene oxide on the carbon electrode (SPCE). The CVs were recorded in PBS (pH 6.5) at potential ranging from 0.1 to −1.2 V vs. Ag/AgCl at a scan rate 50 mV/s for 10 subsequent cycles. The choice of a slightly acidic electrolyte is in line with reports suggesting that the electrochemical reduction of GO occurs at faster kinetics in acidic electrolyte due to the higher concentration of H^+. The presence of H^+ facilitates the removal of oxygen functionalities and simultaneous hydrogenation of the carbon atoms in the graphitic structure [31,32]. On CV (Figure 1A), a broad cathodic peak is observed at potential −0.65 V to −0.96 V, which is attributed to the reduction in oxygen functional groups of GO. On successive cycling, the cathodic peak disappeared, which is attributed to the oxygen moiety reduction at the GO basal planes [27,33]. The absence of the corresponding anodic peak in the CV plots represents the electrochemical reduction of GO being irreversible and the stability of the electrochemically reduced graphene oxide film [30]. To maintain the reproducible electrochemical in-situ reduction, the total observed change in the cathodic current at potential −1.2 V for successive 10 cycles was noted to be 490 µA (±8 µA) for all the fabricated sensors. Cyclic voltammetry (CV) provides valuable information about the electrode surface binding phenomenon during the modifications. We used an electrochemical approach to validate the surface modifications directly in the clean PBS (7.4) without using any redox. Figure 1B represents the typical CV response recorded for control carbon screen-printed electrode (SPCE), GO/SPCE, and rGO/SPCE in the clean PBS (pH 7.4 at scan rate 50 mV/s). No redox probe was used; therefore, after reduction, enhanced capacitive current is observed in the case of the rGO/SPCE compared to control and GO-modified SPCE, confirming removal of oxy functionalities from the GO surface, creating more defects and enhancing electrochemical activity.

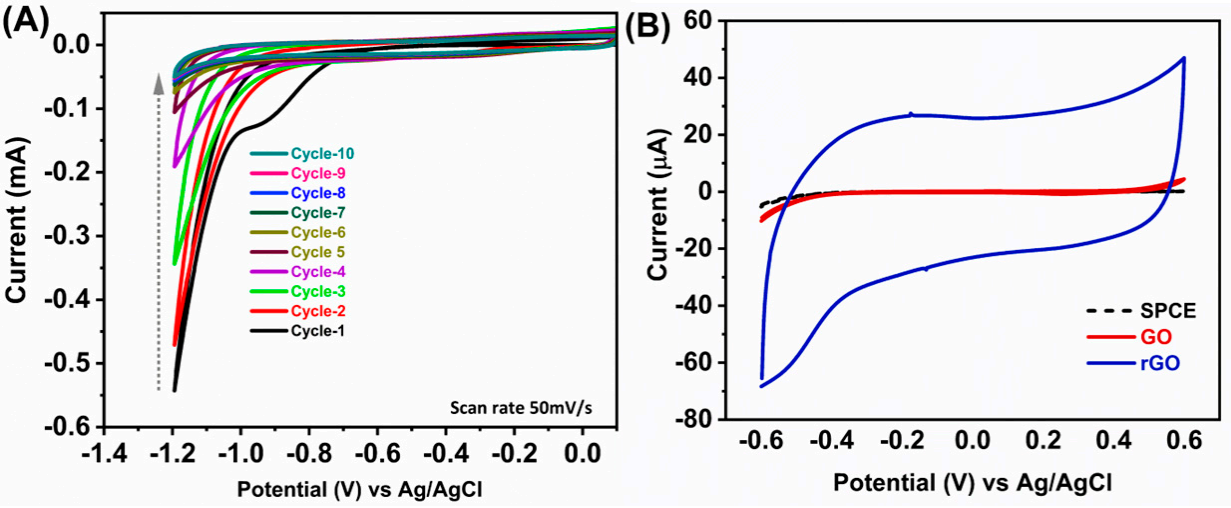


Figure 1. (**A**) Cyclic voltammetry showing in situ electrochemical reduction of GO to rGO on screen-printed carbon electrode (SPCE) in phosphate buffer of pH 6.5. (**B**) Cyclic voltammetry (CV) response recorded for the control SPCE, GO/SPE, and rGO/SPE after reduction in the phosphate-buffered saline (pH 7.4) at a scan rate of 50 mV/s.

Reduced graphene-based materials have been widely explored in sensing applications [28]. The large surface area and enhanced electrochemical activity of rGO compared to bare carbon and GO create an ideal support material for anchoring PQ antibody for our applications [34]. Based on the surface properties and interaction, we chose to use 1-pyrenebutyricacid-N hydroxysuccinimide ester (PANHS), which non-covalently binds to rGO through π–π interaction and promotes the immobilization of the antibodies without affecting the underlying structure [35].

To investigate the molecular interactions during the self-assembly or binding of the antibody onto the cross-linker PANHS-modified rGO/SPE, FTIR spectra were recorded at each step of the modification directly on the sensor [28]. As shown in Figure 2A, for PANHS (commonly known as PBASE) cross-linker-modified rGO/SPE, the absorption peak at 1012 cm^{-1} corresponds to N-O-C esters, while the peaks due to C-N-C stretch of NHS esters group are observed at ~1257 cm^{-1}, 1318 cm^{-1}, 1345 cm^{-1} 1402 cm^{-1} and 1440 cm^{-1}. The peak at 1745 cm^{-1} corresponds to C=O stretching of NHS esters, confirming the binding of the linker to rGO/SPE. The characteristics peak due to carbonyl in PANHS is observed at 1725 cm^{-1}, while the peaks at 1785 and 1816 cm^{-1} correspond to the symmetric and asymmetric stretching vibration of the two carbonyl groups in the imide, and the peak due to C–N stretching vibration is observed at 1375 cm^{-1} [28]. On antibody immobilization, the C-O bond of NHS ester reacts with the primary amines of the antibody, forming stable amides. All the peaks corresponding to the NHS diminish and an enhanced aminolysis peak is observed at 1644 cm^{-1}, confirming the successful binding of the PQ antibody (PQ-Ab) to cross-linker-modified SPE. The surface morphological characterization of the modified immunosensor sensor platform was also confirmed by AFM. Figure 2C,D depict 2D and 3D in-situ images of the PQ antibody-modified rGO surface, respectively, at a resolution of 2 µm. The exfoliated and electrochemically reduced rGO shows lumpy and wrinkled surfaces depicting morphology characteristic of rGO, which can be attributed to the increase in van der Waals forces upon removal of oxygen functionalities during electrochemical reduction [29,32]. The antibody (marked by an arrow) appeared embedded into the cross-linker surface that is adhered to the graphene network, confirming the successful binding of the antibody on the sensor platform [36–38].

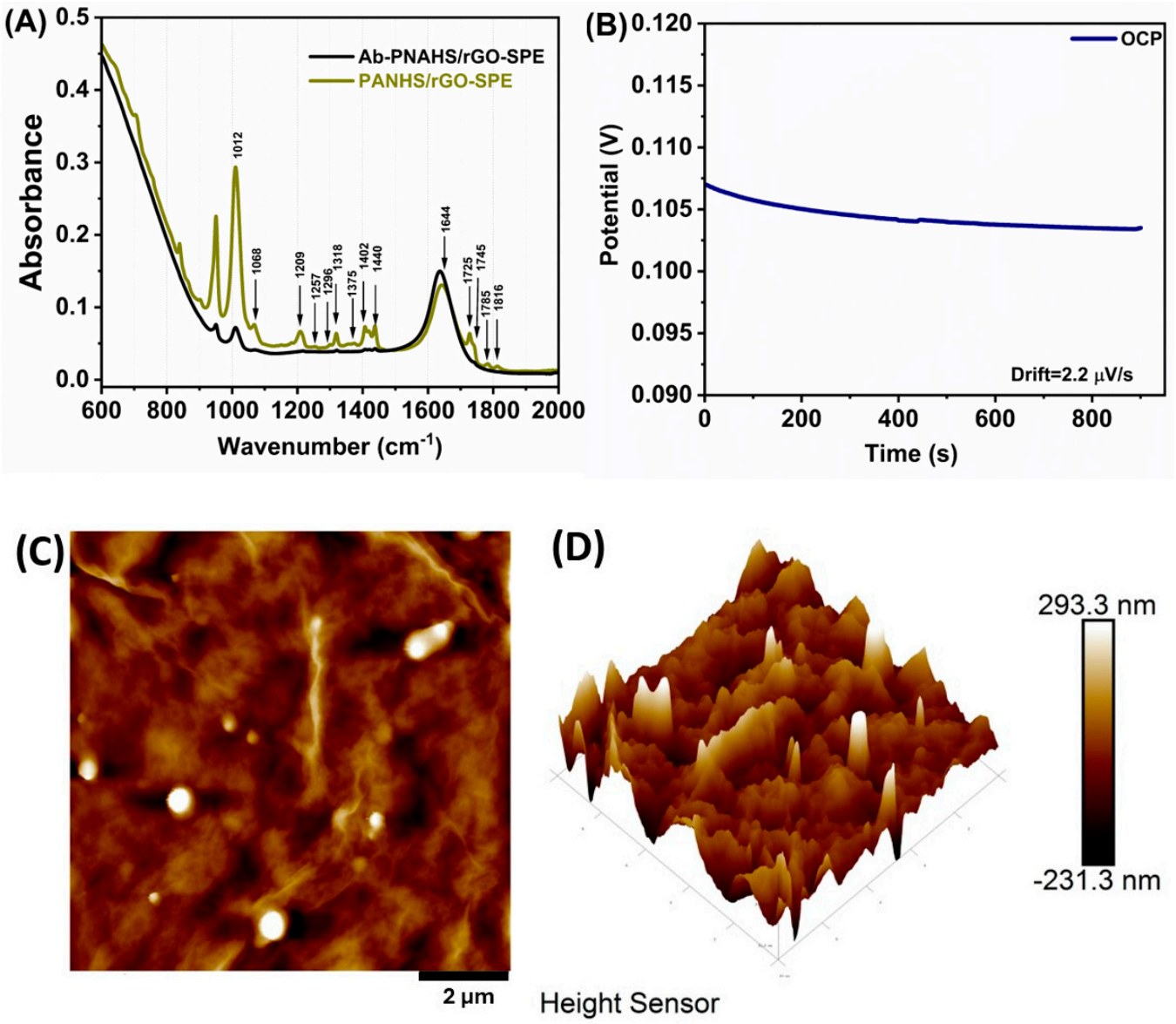


Figure 2. (**A**) FTIR spectra recorded after cross-linker immobilization and anchoring of the paraquat antibody on the surface of rGO/SPCE sensor platform. (**B**) Open circuit potential recorded for the paraquat antibody-modified sensor platform in the test sample recorded for 15 min with the drift observed to be 2.2 µV/s. In-situ AFM images: (**C**) 2D AFM image of the PQ antibody-modified rGO surface showing cross-linker embedded on the graphene surface; (**D**) 3D AFM image of the prepared sensor surface showing surface roughness of the graphene support and equivalent height profile of antibody protruding from the cross-linker surface.

3.2. Electrochemical Detection of Paraquat in Drinking Water Sample

The test sample of interest is pure drinking water. However, the charged minerals in the drinking water greatly interfered with the detection and reproducibility as per initial trial experiments. To avoid this issue, the study was performed by diluting the drinking water with PBS at a 1:1 ratio (50% drinking water and 50% PBS). After successful modification of the sensing platform, the developed (PQ-Ab/rGO-SPCE) sensor was first tested for stability in the test media, which is a water sample, as shown in Figure 2B, as the pH of the test media would influence the performance of the sensor. We performed stability tests of the developed sensor platform in water samples and measured the inherent potential between the working and reference electrodes without any applied bias for a period of 15 min. A stable response was observed with a drift of 2.2 µV/s, and therefore we

chose the incubation time for test samples to be 15 min to allow the system to stabilize. After completing the stability testing of the sensor in the test media, we finally demonstrated our modified sensor platform for the real-life testing of PQ in drinking water samples. Therefore, to test the performance characterization of the immunoassay based modified sensor platform for the detection of PQ, we used the electrochemical method using non-faradaic electrochemical impedance spectroscopy (EIS) at AC bias of 10 mV at a frequency of 10–10^6 Hz.

Electrochemical methods or detection tools have been widely employed in research due to their high sensitivity, fast response, and portable on-field sensing applications. Electrochemical impedance spectroscopy (EIS) is a very powerful technique or tool used to investigate interfacial properties associated with bio-recognition events occurring at the modified electrode surface. The major advantage of EIS is small-amplitude perturbation from steady state, making it a non-destructive tool. Briefly, EIS measurements can be accomplished in two different ways, faradaic EIS, and non-faradaic EIS. The measurements or detection at faradaic EIS are carried out using a redox probe, while in non-faradaic impedance, no redox probe is used [38]. Impedimetric immunosensing is a sensitive technique for simultaneous label-free detection of antigen–antibody binding on the electrode surface. In impedimetric immunosensors, antibodies are immobilized on the electrodes, and responses in non-faradaic electrode modification are monitored by changes in the double-layer capacitance (Cdl). The faradaic configuration with a redox probe in solution, response, and signal are monitored by changes in charge transfer resistance (Rct). On the other hand, for a faradaic interface where the redox probe is confined on the electrode surface, responses are monitored by the changes in redox capacitance (Cr) [38–40]. In our study using immunoassay-based sensor modification, we employed non-faradaic EIS as the measurement tool used to gauge the response of the sensor as a function of the binding of the target antigen (paraquat) to the antibody immobilized on our sensor platform. The idea of our study was to determine the feasibility of our sensor platform to test water samples directly in low volume using an immunoassay-based screen-printed sensor, which was demonstrated using a benchtop potentiostat.

The performance characterization on immunoassay modified sensor platform was achieved by generating a calibrated dose–response plot (CDR) obtained by plotting the electrochemical signal response as a function of the known added spiked concentration doses of PQ in the test sample. The test sample consisted of drinking water and PBS solution at a ratio of 1:1. For the calibrated dose measurement (CDR) test, the drinking water samples were spiked with target PQ at concentrations of ZD (control with no spike), 0.05, 0.1, 0.3, 0.9, 2.7, 8.1, 24.3, and 72.9 ng/mL (0.19, 0.39, 1.17, 3.5, 10.5, 31.5, 94.5, and 283.5 nM, respectively). The CDR range was selected to cover the limit by the United States Environment Protection Agency (US EPA limit of PQ in water at ~0.03 µg/mL or 30 ng/mL). To compare the response of the control sensor (rGO-modified SPE without antibody), a similar test was performed with ZD and 0.1, 0.3, 0.9, 2.7, 8.1 ng/mL of paraquat in water samples. For testing or measurements, the sensor was placed in a Faraday cage, to which 50 µL of the zero dose (ZD/control dose with no spiked PQ antigen) was dispensed on the electrode surface and allowed to incubate for 15 min. A wet tissue was placed inside the Faraday cage to maintain moisture or prevent the drying of the test sample during the prolonged incubation. After the incubation period, EIS measurements were recorded. The zero-dose liquid was then slowly removed from the electrode surface via pipet. The 0.05 ng/mL (50 uL) dose was then dispensed onto the electrode surface and allowed to incubate for 15 min and EIS was recorded. An incubation/reaction time of 15 min was there to allow sufficient binding of the antigens to the electrode surface and was maintained for all the experiments. This procedure was repeated for the subsequent doses of 0.1, 0.3, 0.9, 2.7, 8.1, 24.3 and 72.9 ng/mL from lower to higher in threefold increments in concentrations of spiked PQ doses respectively.

We aimed to demonstrate the detection of the target PQ directly; therefore, no redox probe was used and the response was specifically due to the binding of target PQ to the

antibody-modified sensor. Electrochemical impedance spectroscopy (EIS) is a sensitive electrochemical tool that can gauge the interaction on the antibody-modified electrode sensor platform as a function of binding of the antigen. The double-layer charge modulation at the electrode–electrolyte surface due to the binding of the target PQ antigen to the specific antibody immobilized on the sensor can observed as a signal change with the added spiked antigen concentration [28,41,42].

Figure 3A presents a raw Bode plot obtained from EIS measurements for all the spiked PQ concentrations in water samples. The plot of the Z_{mod} (Ω) value plotted against the frequency (Hz) shows a decrease in the Z_{mod} value from baseline: from 494 (Ω) to 425 (Ω) with the increasing spiked concentrations of the target PQ. The observed decrease in the Z_{mod} response as a function of the increasing PQ is attributed to the increasing binding of the added antigen resulting in the double-layer modulation corresponding to signal variation in the large frequency range tested. A high signal ratio was observed at the frequency of 200 Hz; therefore, the response at the 200 Hz frequency was selected to generate the calibrated dose–response plot. The test performed for the control rGO sensor is presented in Figure S1 (Supplementary Information), where the Bode response is increasing with added concentrations of paraquat (ZD to 0.1 ng/mL and saturation is observed for the remaining doses depicting the charge or bulk solution contribution). Figure 3B presents the CDR plot generated by plotting the percentage change in Z_{mod} from the baseline vs. the spiked concentrations (ng/mL) of the PQ tested in a water sample. The CDR was obtained using six replicates (N = 6) repeated three times for each replicate. The percentage change in Z_{mod} value ranged from 2.03% for 0.05 ng/mL to 11% for the 72.9 ng/mL of the spiked PQ concentrations. The specific signal threshold is depicted by the dotted line in Figure 3B and was calculated by 3 × standard deviation of blank + mean of blank. The limit of detection (LOD) was the first measurable concentration above the SST and the LOD was 0.05 ng/mL was observed for our platform. The graphical mechanism of the sensor platform to detect PQ is shown in Figure 3C using Bode response obtained using non-faradaic EIS. The red dotted line denotes the single-frequency region where CDR plots were obtained, showing flexibility to choose a single-frequency feasibility for portable sensor device output. A comparison of various recently reported sensor platforms for PQ detection is presented in Table S1. Very sensitive detection was reported using PbO-NPs/SPE (LOD of 0.28 µg/L~0.28 ng/mL), SPCE/GO-AuNPs/P3ABA (LOD of 0.116 µg/L~116 ng/mL), CoS_2-GCN/GCE (LOD of 4.13 nM~1 ng/mL). The calibration dose–response (CDR) plots were generated using clean buffer, and then spike and recovery tests were performed [14,43–48].

After generating the calibration plot, the effective performance of our developed sensor in the water sample was demonstrated by performing a spike and recovery study, as shown in Figure 4. In this study, known concentrations (actual concentrations) of PQ spiked in triplicate were compared with the measured concentrations calculated based on the previously developed calibration curve (Figures 3B and 4A). Figure 4A represents the calibration curve of sensor response obtained as a function of the spiked PQ doses in a water sample. The CDR curve was fitted using the non-linear regression model with R^2 = 0.99 (Figure 4A), and the equation was used to calculate the recovered concentration. For the spike and recovery study, we randomly picked five spiked concentrations of PQ—0.1 ng/mL, 1 ng/mL, 2.7 ng/mL, 10 ng/mL and 30 ng/mL (0.38, 3.8, 10.5, 38.9 and 116.6 nM respectively)—and measured their EIS response, then the response was back-calculated to generate recovered concentration using the CDR equation, as shown in Figure 4B. The recovery percentage falls within ±10% to 15% error and the sample tested was of three replicates prepared on different days. The test confirms the performance ability of the sensor below and above the MRL by EPA for water. The gold-standard analytical validation method only confirms the ability to test water samples at concentrations higher than the 10 ng/mL range.

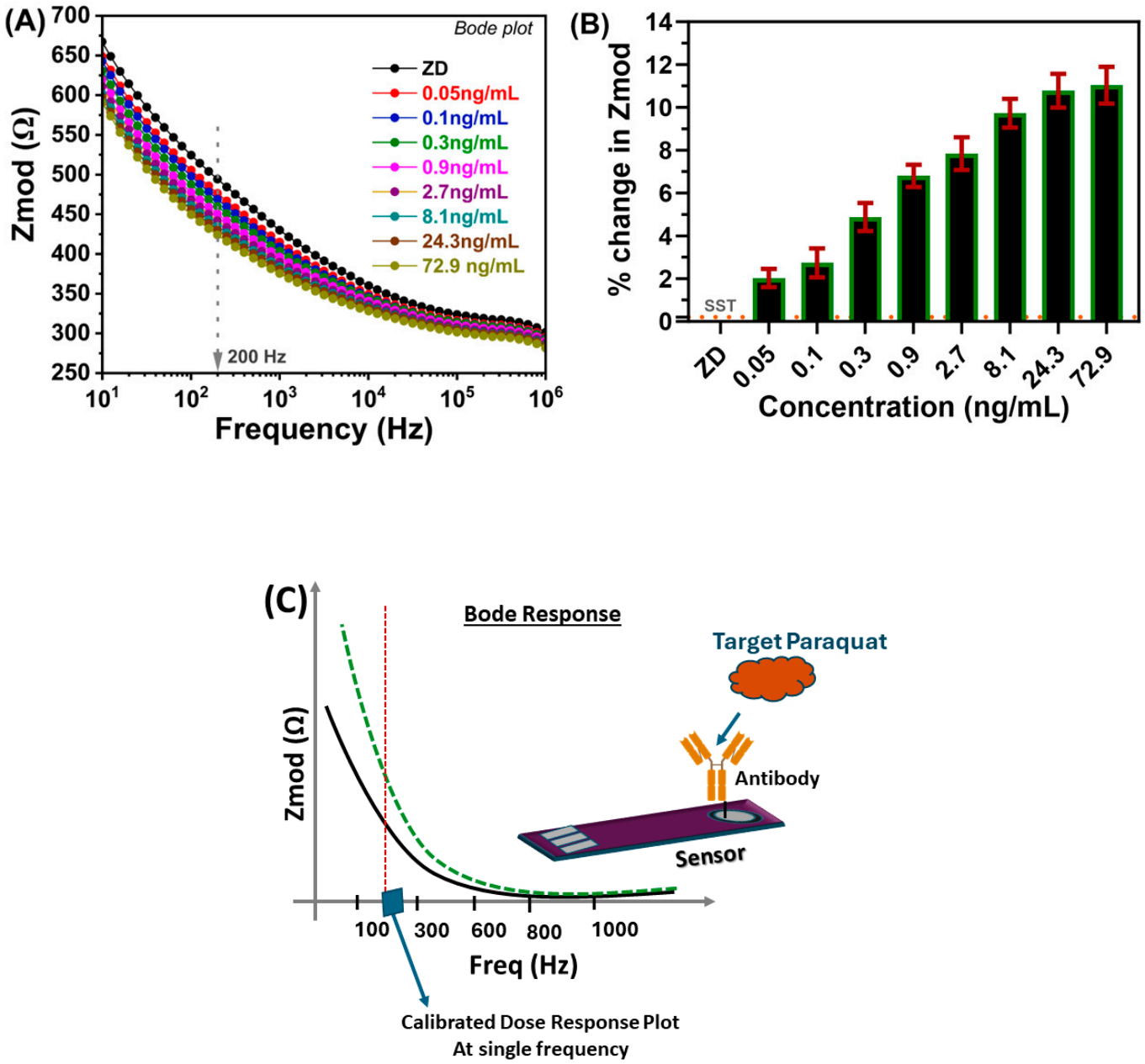


Figure 3. Electrochemical response of the sensor platform. (**A**) Characteristic Bode response observed using developed sensor for the control and spiked concentrations of paraquat in water at concentrations of 0.05–72.9 ng/mL using benchtop electrochemical potentiostat (**B**) Calibrated dose–response (CDR) plot as a function of the spiked concentrations obtained from single frequency. (**C**) Graphical mechanism of PQ detection on modified sensor using Bode response obtained using non-faradaic EIS. The red dotted line demonstrates the single-frequency region where CDR plots were obtained, showing flexibility to choose a single-frequency feasibility for portable sensor device output.

The selectivity of the prepared sensor is crucial in real-time applications when it coexists with structurally similar pesticides found in water samples. Therefore, we tested the sensor platform for cross-reactivity with glyphosate, a common pesticide used widely. The PQ antibody-modified sensor was tested to observe the response of the cross-reactive antigen spiked at doses of 0.1, 0.3, 0.9, 2.7 and 8.1 ng/mL in water samples. As shown in Figure 5A, the lowest glyphosate concentration doses of 0.1 and 0.3 ng/mL showed completely opposite response profiles to the PQ antigen, while higher doses showed a response of 1.8% for 8.1 ng/mL which is 4.5 times lower than the response observed for the

target PQ antigen (8.1%), which confirmed the highly selective performance response of our sensor. For the stability measurements, a batch of five sensors was prepared following the protocol discussed in the sensor fabrication section and were stored in a refrigerator (4 °C). Figure 5B shows responses in a box plot of all the five sensors tested for two spiked concentrations of PQ 0.3 ng/mL and 24.3 ng/mL. The response percentage was within <20% error, confirming the stability of the prepared sensors.

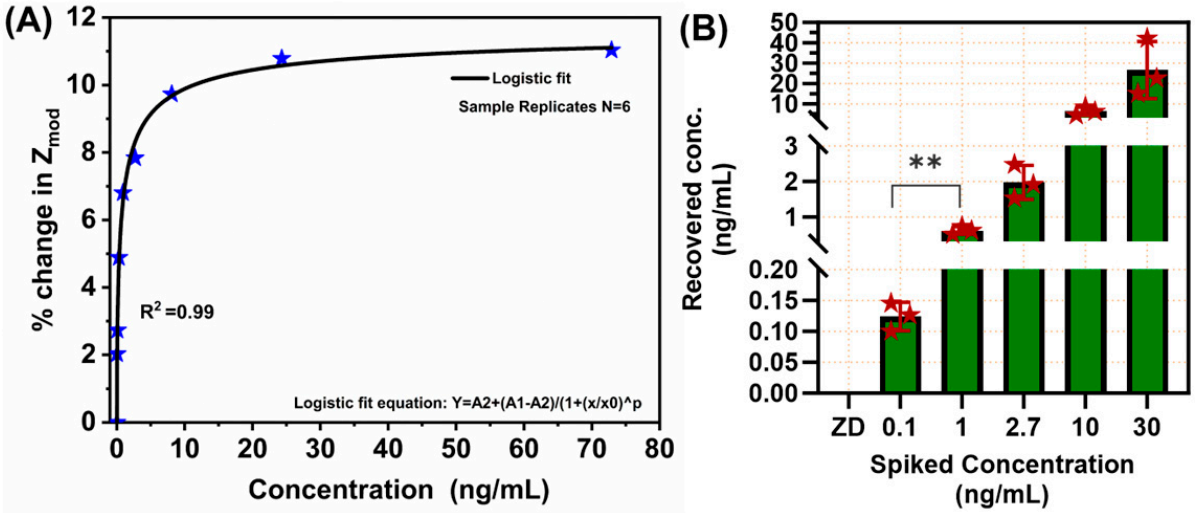


Figure 4. Electrochemical performance of the sensor. (**A**) Calibrated dose–response plot obtained for the spiked concentration doses of paraquat from ZD and 0.05 ng/mL to 72.9 ng/mL in water samples. (**B**) Spike and recovery data obtained using the sensor platform. ** Significance difference between two lower concentrations, 0.1 ng/ mL and 1 ng/mL (** $p < 0.01$).

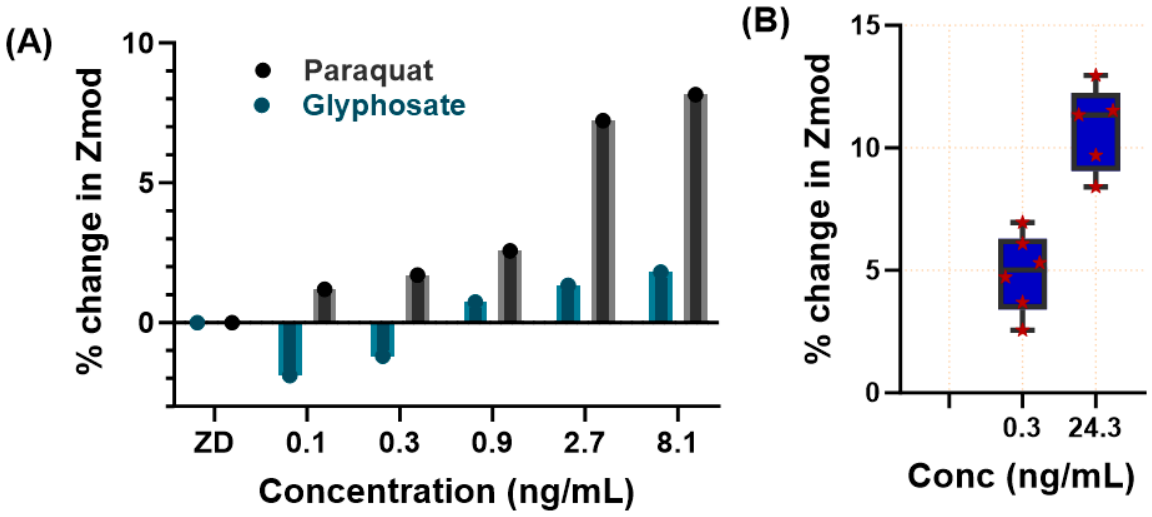


Figure 5. (**A**) Cross-reactivity on PQ-Ab/rGO-SPCE sensor with glyphosate antigen and comparison of the response with target paraquat. (**B**) Stability of developed sensor over 5 days represented in box plots showing distribution of the points .

4. Conclusions

In this study, we successfully demonstrated an antibody-modified (PQ-Ab/rGO-SPCE) electrochemical sensor platform for the testing of PQ directly in drinking water samples. The sensor showed a wide response range, with a limit of detection (LOD) as low as 0.05 ng/mL (0.19 nM). This unique combination of carbon-based support with the antibody specific to the target antigen helped to capture or detect the PQ antigen directly without sample preprocessing using the electrochemical method within 15 min. The selectivity of

the sensor was tested against glyphosate, and high stability was observed for a period of 5 days. This is a successful first-time demonstration of calibrated dose response and spike and recovery directly of PQ in drinking water samples using an immunoassay-based chip sensor at single frequencies. Utilizing a low sample volume with direct detection and the ability to capture responses in a single frequency opens the possibility of applying this platform to portable electrochemical on-field sensor technology.

Supplementary Materials: The following supporting information can be downloaded at: https://www.mdpi.com/article/10.3390/electrochem5030022/s1, Figure S1: Characteristic bode response observed for test performed using control rGO sensor for the paraquat concentrations ZD, 0.1, 0.3, 0.9, 2.7 and 8.1 ng/mL in water sample; Table S1: Comparison of the reported and developed electrochemical sensor for the determination of Paraquat (PQ).

Author Contributions: Conceptualization, D.C.P.,V.N.D., S.M. (Sriram Muthukumar) and S.P.; methodology, D.C.P., V.N.D., S.M. (Sriram Muthukumar) and S.P.; software, D.C.P. and V.N.D.; validation, D.C.P., M.S., S.M. (Sera Mohammed), C.N.T., A.P. and D.B.; formal analysis, D.C.P. and M.S.; investigation, D.C.P., V.N.D., S.M. (Sriram Muthukumar) and S.P.; resources, S.M. (Sriram Muthukumar) and S.P.; data curation, D.C.P.; writing—original draft preparation, D.C.P. and M.S.; writing—review and editing, D.C.P., V.N.D., S.M. (Sriram Muthukumar) and S.P.; visualization, D.C.P.; supervision, S.M. (Sriram Muthukumar) and S.P.; project administration, S.P.; funding acquisition, S.P. All authors have read and agreed to the published version of the manuscript.

Funding: This research received no external funding.

Institutional Review Board Statement: Not applicable.

Informed Consent Statement: Not applicable.

Data Availability Statement: Data supporting the reported results are contained within the article and Supplementary Materials. No new data were created beyond those presented in the study.

Acknowledgments: The authors would like to thank Anirban Paul for the help with AFM characterization.

Conflicts of Interest: The authors declare the following competing financial interest(s): Shalini Prasad and Sriram Muthukumar have a significant interest in Enlisense LLC, a company that may have a commercial interest in the results of this research and technology. The potential individual conflict of interest has been reviewed and managed by The University of Texas at Dallas, and played no role in the study design; in the collection, analysis, and interpretation of data; in the writing of the report, or in the decision to submit the report for publication.

References

1. Thimoonnee, S.; Somnet, K.; Ngaosri, P.; Chairam, S.; Karuwan, C.; Kamsong, W.; Tuantranont, A.; Amatatongchai, M. Fast, Sensitive and Selective Simultaneous Determination of Paraquat and Glyphosate Herbicides in Water Samples Using a Compact Electrochemical Sensor. *Anal. Methods* **2022**, *14*, 820–833. [CrossRef]
2. Zhang, J.; Lin, Z.; Qin, Y.; Li, Y.; Liu, X.; Li, Q.; Huang, H. Fabricated Electrochemical Sensory Platform Based on the Boron Nitride Ternary Nanocomposite Film Electrode for Paraquat Detection. *ACS Omega* **2019**, *4*, 18398–18404. [CrossRef]
3. de Figueiredo-Filho, L.C.S.; Baccarin, M.; Janegitz, B.C.; Fatibello-Filho, O. A Disposable and Inexpensive Bismuth Film Minisensor for a Voltammetric Determination of Diquat and Paraquat Pesticides in Natural Water Samples. *Sens. Actuators B Chem.* **2017**, *240*, 749–756. [CrossRef]
4. Valera, E.; García-Febrero, R.; Pividori, I.; Sánchez-Baeza, F.; Marco, M.P. Coulombimetric Immunosensor for Paraquat Based on Electrochemical Nanoprobes This Work Is Dedicated to the Memory of Dr. Francisco Sanchez-Baeza. *Sens. Actuators B Chem.* **2014**, *194*, 353–360. [CrossRef]
5. Li, M.; Wang, X.; Zhu, Y.; Jia, X.; Zhang, S.; Wang, H.; Li, Y.; Hu, G. Fe_2O_3-Decorated Boron/Nitrogen-Co-Doped Carbon Nanosheets as an Electrochemical Sensing Platform for Ultrasensitive Determination of Paraquat in Natural Water. *Chin. Chem. Lett.* **2023**, *34*, 2–7. [CrossRef]
6. Rial-Otero, R.; Cancho-Grande, B.; Perez-Lamela, C.; Simal-Gándara, J.; Arias-Estévez, M. Simultaneous Determination of the Herbicides Diquat and Paraquat in Water. *J. Chromatogr. Sci.* **2006**, *44*, 539–542. [CrossRef]
7. Hara, S.; Sasaki, N.; Takase, D.; Shiotsuka, S.; Ogata, K.; Futagami, K.; Tamura, K. Rapid and Sensitive HPLC Method for the Simultaneous Determination of Paraquat and Diquat in Human Serum. *Anal. Sci.* **2007**, *23*, 523–526. [CrossRef]

8. Kamkrua, N.; Ngernsutivorakul, T.; Limwichean, S.; Eiamchai, P.; Chananonnawathorn, C.; Pattanasetthakul, V.; Ricco, R.; Choowongkomon, K.; Horprathum, M.; Nuntawong, N.; et al. Au Nanoparticle-Based Surface-Enhanced Raman Spectroscopy Aptasensors for Paraquat Herbicide Detection. *ACS Appl. Nano Mater.* **2023**, *6*, 1072–1082. [CrossRef]
9. Wachholz Junior, D.; Deroco, P.B.; Kubota, L.T. A Copper-Based Metal-Organic Framework/Reduced Graphene Oxide-Modified Electrode for Electrochemical Detection of Paraquat. *Microchim. Acta* **2022**, *189*, 278. [CrossRef]
10. Poudyal, D.C.; Dhamu, V.N.; Samson, M.; Muthukumar, S.; Prasad, S. Portable Pesticide Electrochem-Sensor: A Label-Free Detection of Glyphosate in Human Urine. *Langmuir* **2022**, *38*, 1781–1790. [CrossRef]
11. Poudyal, D.C.; Satpati, A.K.; Kumar, S.; Haram, S.K. High Sensitive Determination of Dopamine through Catalytic Oxidation and Preconcentration over Gold-Multiwall Carbon Nanotubes Composite Modified Electrode. *Mater. Sci. Eng. C* **2019**, *103*, 109788. [CrossRef] [PubMed]
12. Banga, I.; Paul, A.; Poudyal, D.C.; Muthukumar, S.; Prasad, S. Recent Advances in Gas Detection Methodologies with a Special Focus on Environmental Sensing and Health Monitoring Applications–A Critical Review. *ACS Sens.* **2023**, *8*, 3307–3319. [CrossRef] [PubMed]
13. Dhamu, V.N.; Poudyal, D.; Samson, M.; Paul, A.; Muthukumar, S.; Prasad, S. Review—Environmental Biosensors for Agro-Safety Based on Electrochemical Sensing Mechanism with an Emphasis on Pesticide Screening. *ECS Sens. Plus* **2023**, *2*, 024601. [CrossRef]
14. Traiwatcharanon, P.; Siriwatcharapiboon, W.; Jongprateep, O.; Wongchoosuk, C. Electrochemical Paraquat Sensor Based on Lead Oxide Nanoparticles. *RSC Adv.* **2022**, *12*, 16079–16092. [CrossRef]
15. Jiang, Y.; Li, Q.; Yao, J.; Guo, X.; Ying, Y.; Liu, X.; Wen, Y.; Yang, H.; Wu, Y. Advanced Photoelectrochemical Detection of Paraquat Based on Plasmonic Metal Modified Photocathode Material. *Appl. Surf. Sci.* **2022**, *581*, 151903. [CrossRef]
16. Sant'Anna, M.V.S.; Silva, J.d.O.S.; Gevaerd, A.; Lima, L.S.; Monteiro, M.D.S.; Carregosa, I.S.C.; Wisniewski, A.; Marcolino-Junior, L.H.; Bergamini, M.F.; Sussuchi, E.M. Selective Carbonaceous-Based (Nano)Composite Sensors for Electrochemical Determination of Paraquat in Food Samples. *Food Chem.* **2022**, *373*, 131521. [CrossRef]
17. Zheng, W.; Su, R.; Yu, G.; Liu, L.; Yan, F. Highly Sensitive Electrochemical Detection of Paraquat in Environmental Water Samples Using a Vertically Ordered Mesoporous Silica Film and a Nanocarbon Composite. *Nanomaterials* **2022**, *12*, 3632. [CrossRef]
18. Liang, G.; He, Z.; Zhen, J.; Tian, H.; Ai, L.; Pan, L.; Gong, W. Development of the Screen-Printed Electrodes: A Mini Review on the Application for Pesticide Detection. *Environ. Technol. Innov.* **2022**, *28*, 102922. [CrossRef]
19. Pilas, J.; Selmer, T.; Keusgen, M.; Schöning, M.J. Screen-Printed Carbon Electrodes Modified with Graphene Oxide for the Design of a Reagent-Free NAD+-Dependent Biosensor Array. *Anal. Chem.* **2019**, *91*, 15293–15299. [CrossRef]
20. Li, J.; Lei, W.; Xu, Y.; Zhang, Y.; Xia, M.; Wang, F. Fabrication of Polypyrrole-Grafted Nitrogen-Doped Graphene and Its Application for Electrochemical Detection of Paraquat. *Electrochim. Acta* **2015**, *174*, 464–471. [CrossRef]
21. Hamilton, D.J.; Ambrus, Á.; Dieterle, R.M.; Felsot, A.S.; Harris, C.A.; Holland, P.T.; Katayama, A.; Kurihara, N.; Linders, J.; Unsworth, J.; et al. Regulatory Limits for Pesticide Residues in Water (IUPAC Technical Report). *Pure Appl. Chem.* **2003**, *75*, 1123–1155. [CrossRef]
22. Dos Santos, L.B.O.; Infante, C.M.C.; Masini, J.C. Development of a Sequential Injection-Square Wave Voltammetry Method for Determination of Paraquat in Water Samples Employing the Hanging Mercury Drop Electrode. *Anal. Bioanal. Chem.* **2010**, *396*, 1897–1903. [CrossRef]
23. Li, Y.; Liu, L.; Kuang, H.; Xu, C. Preparing Monoclonal Antibodies and Developing Immunochromatographic Strips for Paraquat Determination in Water. *Food Chem.* **2020**, *311*, 125897. [CrossRef] [PubMed]
24. Garcia-Febrero, R.; Salvador, J.P.; Sanchez-Baeza, F.; Marco, M.P. Rapid Method Based on Immunoassay for Determination of Paraquat Residues in Wheat, Barley and Potato. *Food Control* **2014**, *41*, 193–201. [CrossRef]
25. Benvidi, A.; Tezerjani, M.D.; Jahanbani, S.; Mazloum Ardakani, M.; Moshtaghioun, S.M. Comparison of Impedimetric Detection of DNA Hybridization on the Various Biosensors Based on Modified Glassy Carbon Electrodes with PANHS and Nanomaterials of RGO and MWCNTs. *Talanta* **2016**, *147*, 621–627. [CrossRef] [PubMed]
26. Guo, H.L.; Wang, X.F.; Qian, Q.Y.; Wang, F.B.; Xia, X.H. A Green Approach to the Synthesis of Graphene Nanosheets. *ACS Nano* **2009**, *3*, 2653–2659. [CrossRef]
27. Ibáñez-Redín, G.; Wilson, D.; Gonçalves, D.; Oliveira, O.N. Low-Cost Screen-Printed Electrodes Based on Electrochemically Reduced Graphene Oxide-Carbon Black Nanocomposites for Dopamine, Epinephrine and Paracetamol Detection. *J. Colloid Interface Sci.* **2018**, *515*, 101–108. [CrossRef] [PubMed]
28. Poudyal, D.C.; Dhamu, V.N.; Samson, M.; Malik, S.; Kadambathil, C.S.; Muthukumar, S.; Prasad, S. How Safe Is Our Food We Eat? An Electrochemical Lab-on-Kitchen Approach towards Combinatorial Testing for Pesticides and GMOs; A Case Study with Edamame. *Ecotoxicol. Environ. Saf.* **2023**, *252*, 114635. [CrossRef]
29. Shao, Y.; Wang, J.; Engelhard, M.; Wang, C.; Lin, Y. Facile and Controllable Electrochemical Reduction of Graphene Oxide and Its Applications. *J. Mater. Chem.* **2010**, *20*, 743–748. [CrossRef]
30. Zhou, A.; Bai, J.; Hong, W.; Bai, H. Electrochemically Reduced Graphene Oxide: Preparation, Composites, and Applications. *Carbon* **2022**, *191*, 301–332. [CrossRef]
31. Quezada-Renteria, J.A.; Ania, C.O.; Chazaro-Ruiz, L.F.; Rangel-Mendez, J.R. Influence of Protons on Reduction Degree and Defect Formation in Electrochemically Reduced Graphene Oxide. *Carbon* **2019**, *149*, 722–732. [CrossRef]

32. Pandey, S.K.; Sachan, S.; Singh, S.K. Electrochemically Reduced Graphene Oxide Modified with Electrodeposited Thionine and Horseradish Peroxidase for Hydrogen Peroxide Sensing and Inhibitive Measurement of Chromium. *Mater. Sci. Energy Technol.* **2019**, *2*, 676–686. [CrossRef]
33. Deng, K.Q.; Zhou, J.h.; Li, X.F. Direct Electrochemical Reduction of Graphene Oxide and Its Application to Determination of L-Tryptophan and l-Tyrosine. *Colloids Surf. B Biointerfaces* **2013**, *101*, 183–188. [CrossRef]
34. Pavlidis, I.V.; Patila, M.; Bornscheuer, U.T.; Gournis, D.; Stamatis, H. Graphene-Based Nanobiocatalytic Systems: Recent Advances and Future Prospects. *Trends Biotechnol.* **2014**, *32*, 312–320. [CrossRef] [PubMed]
35. Sethi, J.; Van Bulck, M.; Suhail, A.; Safarzadeh, M.; Perez-Castillo, A.; Pan, G. A Label-Free Biosensor Based on Graphene and Reduced Graphene Oxide Dual-Layer for Electrochemical Determination of Beta-Amyloid Biomarkers. *Microchim. Acta* **2020**, *187*, 288. [CrossRef]
36. Iijima, M.; Somiya, M.; Yoshimoto, N.; Niimi, T.; Kuroda, S. Nano-Visualization of Oriented-Immobilized IgGs on Immunosensors by High-Speed Atomic Force Microscopy. *Sci. Rep.* **2012**, *2*, 790. [CrossRef]
37. Gao, Z.; Ducos, P.; Ye, H.; Zauberman, J.; Sriram, A.; Yang, X.; Wang, Z.; Mitchell, M.W.; Lekkas, D.; Brisson, D.; et al. Graphene Transistor Arrays Functionalized with Genetically Engineered Antibody Fragments for Lyme Disease Diagnosis. *2D Mater.* **2020**, *7*, 024001. [CrossRef]
38. Coppari, E.; Santini, S.; Bizzarri, A.R.; Cannistraro, S. Kinetics and Binding Geometries of the Complex between B2-Microglobulin and Its Antibody: An AFM and SPR Study. *Biophys. Chem.* **2016**, *211*, 19–27. [CrossRef]
39. Daniels, J.S.; Pourmand, N. Label-Free Impedance Biosensors: Opportunities and Challenges. *Electroanalysis* **2007**, *19*, 1239–1257. [CrossRef]
40. Kazemi, S.H.; Shanehsaz, M.; Ghaemmaghami, M. Non-Faradaic Electrochemical Impedance Spectroscopy as a Reliable and Facile Method: Determination of the Potassium Ion Concentration Using a Guanine Rich Aptasensor. *Mater. Sci. Eng. C* **2015**, *52*, 151–154. [CrossRef]
41. Tkac, J.A.N.; Davis, J.J. Label-Free Field Effect Protein Sensing. In *Engineering the Bioelectronic Interface: Applications to Analyte Biosensing and Protein Detection*; Royal Society of Chemistry: Cambridge, UK, 2009; ISBN 9781847559777.
42. Lisdat, F.; Schäfer, D. The Use of Electrochemical Impedance Spectroscopy for Biosensing. *Anal. Bioanal. Chem.* **2008**, *391*, 1555–1567. [CrossRef]
43. Pimalai, D.; Putnin, T.; Bamrungsap, S. A Highly Sensitive Electrochemical Sensor Based on Poly(3-Aminobenzoic Acid)/Graphene Oxide-Gold Nanoparticles Modified Screen Printed Carbon Electrode for Paraquat Detection. *J. Environ. Sci.* **2025**, *148*, 139–150. [CrossRef] [PubMed]
44. Yuan, C.; Tang, C.; Zhan, X.; Zhou, M.; Zhang, L.; Chen, W.T.; Abdukayum, A.; Hu, G. ZIF-67 Based CoS2 Self-Assembled on Graphitic Carbon Nitride Microtubular for Sensitive Electrochemical Detection of Paraquat in Fruits. *J. Hazard. Mater.* **2024**, *467*, 133715. [CrossRef]
45. Charoenkitamorn, K.; Chotsuwan, C.; Chaiyo, S.; Siangproh, W.; Chailapakul, O. A New Ready-to-Use Gel-Based Electrolyte for Paraquat Sensor. *Sens. Actuators B Chem.* **2020**, *315*, 128089. [CrossRef]
46. Pacheco, M.R.; Barbosa, S.C.; Quadrado, R.F.N.; Fajardo, A.R.; Dias, D. Glassy Carbon Electrode Modified with Carbon Black and Cross-Linked Alginate Film: A New Voltammetric Electrode for Paraquat Determination. *Anal. Bioanal. Chem.* **2019**, *411*, 3269–3280. [CrossRef] [PubMed]
47. Zhou, H.; Wang, Y.; Xu, L.; Zhou, Y.; Hong, Y.; Hou, D.; Liao, X. Facile Preparation of Ultra Stable Polymer-Based Sensor for Highly Sensitive and Selective Detection of Paraquat in Agricultural Products. *Microchem. J.* **2024**, *199*, 110097. [CrossRef]
48. Ribeiro, J.A.; Carreira, C.A.; Lee, H.J.; Silva, F.; Martins, A.; Pereira, C.M. Voltammetric Determination of Paraquat at DNA-Gold Nanoparticle Composite Electrodes. *Electrochim. Acta* **2010**, *55*, 7892–7896. [CrossRef]

Disclaimer/Publisher's Note: The statements, opinions and data contained in all publications are solely those of the individual author(s) and contributor(s) and not of MDPI and/or the editor(s). MDPI and/or the editor(s) disclaim responsibility for any injury to people or property resulting from any ideas, methods, instructions or products referred to in the content.